Morphology and Crystalline Transition of Poly(3-butylthiophene) Associated with Its Polymorphic Modifications

Guanghao Lu, Ligui Li, and Xiaoniu Yang*

State Key Laboratory of Polymer Physics and Chemistry, Changchun Institute of Applied Chemistry, Chinese Academy of Sciences, Graduate School of the Chinese Academy of Sciences, Renmin Str. 5625, Changchun 130022, P. R. China

Received November 29, 2007; Revised Manuscript Received January 10, 2008

ABSTRACT: Poly(3-butylthiophene) (P3BT) is a much less studied conjugated polymer despite its high crystallizability and thus excellent electrical property. In this work, morphology of P3BT at different crystalline polymorphs and solvent/thermal induced phase transition between form I and II modifications have been intensively investigated by using optical microscopy, electron microscopy, differential scanning calorimetry, and X-ray diffraction. It is shown that a direct deposition from carbon disulfide (CS_2) at fast evaporation results in P3BT crystals in form I modification, giving typical whiskerlike morphology. In contrast, low evaporation rate from CS_2 leads to formation of form II crystals with spherulitic morphology, which is so far scarcely observed in polythiophene. We further show the crystalline transition of P3BT crystals from form I to II modification upon controlled solvent vapor treatment (C-SVT), in which both the transition rate and the size of the spherulite obtained depend on the vapor pressure and treatment time, respectively. We ascribe the driving force for this transition to the stability differennce of these two modifications in CS_2. However, form II transfers reversely back to form I at about 159 °C via a solid−solid phase transition at elevated temperature. The transition behaviors of P3BT crystals upon both solvent vapor treatment and thermal heating at its bulk state reveals that form II instead of far more commonly observed form I modification is the thermodynamically stable structure for P3BT at room temperature.

Introduction

Conjugated polymers have attracted great attention for their potential applications in inexpensive organic electronic devices by using solvent-based thin film deposition technology.[1−5] Poly(3-alkylthiophene) (P3AT), as an important p-type semiconducting polymer with high crystallizability, has been widely used in field-effect transistors (FET),[2,6] polymer solar cells,[7,8] and so on. For instance, polymer FETs based on poly(3-hexylthiophene) (P3HT) show very promising performance in both mobility and on−off ratio.[2,9,10] P3HT is also one of the most important electron donor materials in high-performance polymer solar cells, of which a power conversion efficiency as high as 4.4%−6.5% has been recently reported by a few groups.[11,12]

For another key member also in the same P3AT family,[13,14] poly(3-butylthiophene) (P3BT), however, is much less studied compared with P3HT. The main reason is due to its poor solubility in the common organic solvents and is thus difficult to perform film deposition for the fabrication of thin film devices. Nevertheless, because of its shorter alkyl substitute on the main backbone, its electrical conductivity and thus free charge carrier mobility should be higher than other polythiophenes with longer side chains.[15−17] Recently, we have reported that P3BT could be easily dissolved in CS_2,[18] which paves the way for its potential applications in many thin film devices since the preparation of the solution with enough concentration for thin film deposition has been overcome. Our further investigation shows that, as a good solvent, CS_2 is able to induce P3BT to form crystals in a thin film with completely different morphology from those typical whiskerlike crystals obtained via using the other solvents. As a consequence, lamellar crystals having ∼15 nm in height and 30−40 nm in width were successfully created in the film, in contrast to the usually observed P3AT whiskers with only ∼5 and ∼15 nm for height and width,[19−21] respectively. In particular, these P3BT lamellae adopt a flat-on orientation with respect to the substrates.[18]

Polymorphism of polythiophene at its crystalline state has been found on regioregular P3ATs with longer side chains[22−24] such as poly(3-octylthiophene) and poly(3-decylthiophene) resulted mainly from the strong packing tendency of long substituted alkyl segment. There are two modifications, i.e., forms I and II associated with P3AT crystals. The main crystallographic difference between these two crystalline polymorphs is the shorter *a*-axis repeat distance of form II compared with that of form I, which is attributed to interdigitation or tilting of the side chains.[22−25] However, prior to our previous publication,[18] no form II has been explicitly obtained from P3AT with short alkyl group like P3BT, due mainly to the too weak interaction between the short butyl substitute segments. Nevertheless, as a highly crystallizable conjugated polymer, the morphology and crystallization behaviors of P3BT, which play a key role in determining its property (functionality) for thin film device applications, are still less understood.

On the basis of our previous work, in this paper we systematically studied various processes which could result in the thin P3BT film with different morphology and crystalline structure as well as phase transition from conventional form I to II upon solvent vapor treatment and reverse transition from form II to I at elevated temperature by using optical microscopy, electron microscopy, differential scanning calorimetry and X-ray diffraction. We could eventually conclude that form II, instead of much more commonly observed form I, is the thermodynamically stable phase at room temperature.

* Corresponding author. E-mail: xnyang@ciac.jl.cn.

10.1021/ma7026512 CCC: $40.75 © 2008 American Chemical Society
Published on Web 02/22/2008

Scheme 1. Setup Used for Controlled Solvent Vapor Treatment (C-SVT)[a]

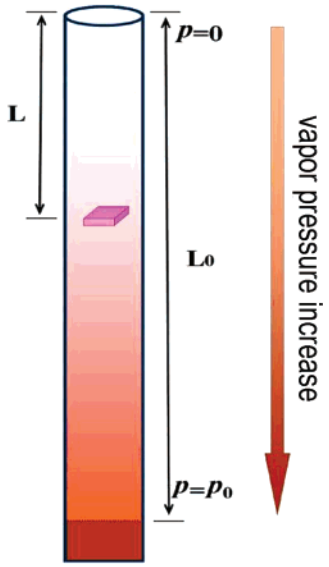

[a] L_0 is the effective length given by distance from the up edge of the setup to the surface of the solvent at the bottom of the tube. The actual value of L_0 in this work is 120 cm so as to achieve a stable and highly resolved gradient of solvent vapor pressure p. L is the distance from the up edge of the setup to the specimen position. Solvent vapor pressure is given by $p = L/L_0$, where $p = 1$ means saturated vapor pressure p_0 at a given temperature.

Experimental Section

Materials. Regioregular poly(3-butylthiophene) (P3BT) (97% head-to-tail regioregular conformation, M_w = 39.4 kDa and polydispersion distribution index (PDI) of 2.29) was purchased from Rieke Metals, Inc. Carbon disulfide (CS_2) was purchased from Sinopharm Chemical Reagent Co. Ltd. *o*-Dichlorobenzene (ODCB, anhydrous, 99%) was purchased from Sigma-Aldrich Co.

Thin Film Specimen Preparation from CS_2 Solution. Thin P3BT films were deposited from P3BT/CS_2 solution with P3BT concentration of 10 mg/mL through either the spin-coating or drop-casting method. Spin-coating (using Laurell Spin Processor WS-400B 6NPP Lite) was conducted on the precleaned glass cover slides as the substrates under ambient atmosphere. A rotation speed within 500−1000 rpm was used to achieve the thin film with thickness of ~120 nm. Drop-casting from the same P3BT/CS_2 solution was performed on precleaned glass cover slides (for optical microscopy and TEM) or silicon wafers (for WAXD) under ambient atmosphere or in a Petri dish with preplaced drops of CS_2 solvent so as to control the solvent evaporation rate via adjusting the amount of CS_2 inside.

Controlled Solvent Vapor Treatment (C-SVT). The thin films for C-SVT experiments were prepared by using *o*-dichlorobenzene (ODCB) as the solvent. P3BT is dissolved in ODCB at 80 °C by stirring for 30 min. Thus prepared and cooled solution to room temperature is used for thin film deposition via spin-coating method aforementioned.

For the experiment of controlled solvent vapor treatment (C-SVT), the pristine films were dipped into a long glass tube (6 cm in diameter and 120 cm in length) containing solvent carbon disulfide at the bottom, as shown in Scheme 1. Upon achieving an equilibrium state through the diffusion of solvent vapor within the tube, a gradient distribution of solvent vapor pressure along the tube will be constructed, from saturated pressure at the bottom to close to zero at the top. Therefore, all the process was paid much attention so as to avoid interrupting too much to the vapor diffusion equilibrium in the tube. After C-SVT, the film was dried in vacuum

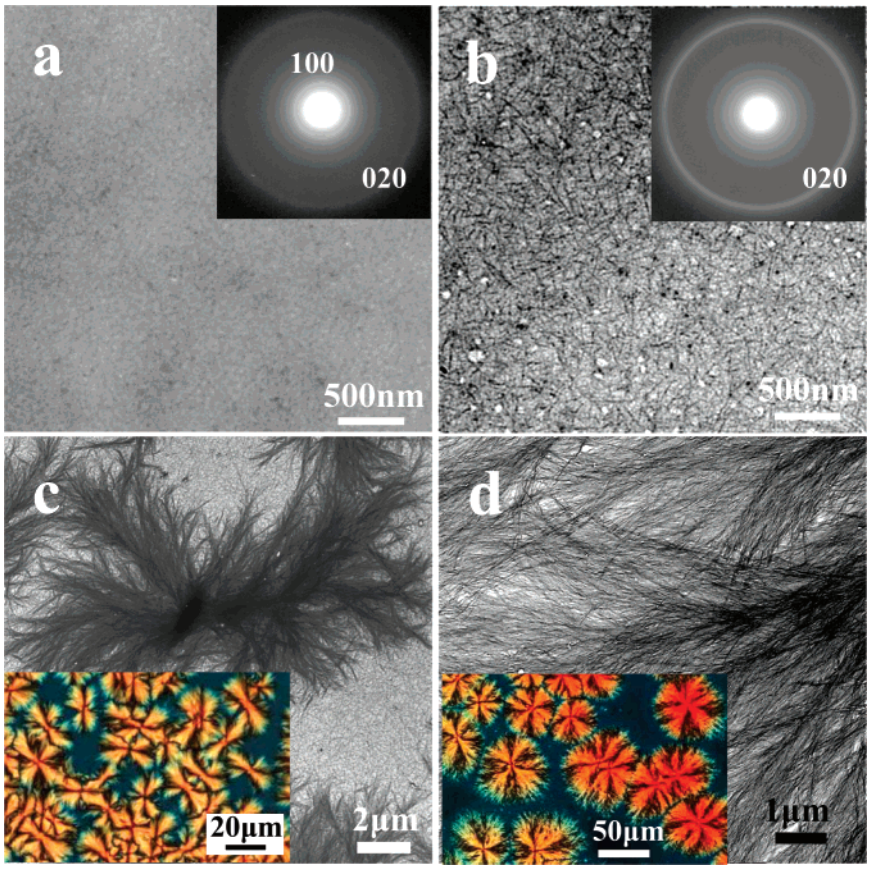

Figure 1. Bright-field transmission electron microscopy (BF-TEM) images showing morphology of thin P3BT film directly deposited from CS_2 solution at different solvent evaporation rates: (a) spin-coated from its CS_2 solution; (b−d) drop-cast from CS_2 solution with an evaporation time of (b) ~5 s, (c) 5 min, and (d) 30 min. Insets of (a, b) and (c, d) are selected-area electron diffraction (SAED) patterns and cross-polarized optical microscopy images, respectively.

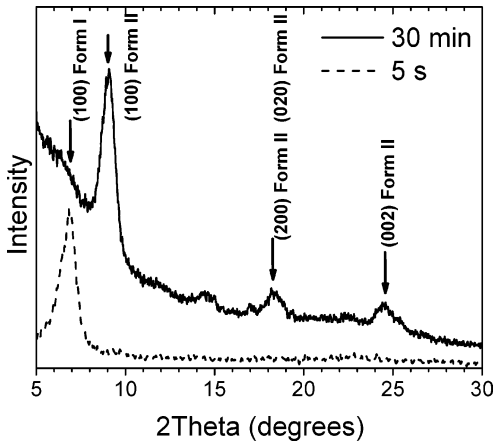

Figure 2. WAXD profiles of thin P3BT films deposited from CS_2 solution with different solvent evaporation times.

at room temperature for 24 h to remove residual solvent in the film.

Characterizations. Wide-angle X-ray diffraction (WAXD) profiles were obtained by using Bruker D8 Discover Reflector with X-ray generation power of 40 kV tube voltage and 40 mA tube current. The diffraction was recorded at a $\theta-2\theta$ symmetry scanning mode with scan angle 2θ within the range of 5°−30°.

TEM was performed on a JEOL JEM-1011 transmission electron microscope operated at 100 kV. Thin films were first floated on deionized water and then transferred onto copper grid. The samples were dried at room temperature for 24 h before TEM experiments.

Polarized optical microscopy (POM) investigations were carried out by a Carl Zeiss A1m microscope.

Scanning electron microscopy (SEM) was performed on a XL30 ESEM-FEG, FEI Co.

DSC curves were performed on TA Q100 DSC, both the heating and cooling rates were set to 10 °C/min.

Results and Discussion

1. Morphology and Crystal Structure of P3BT Prepared from CS_2 Solution through Different Solvent Evaporation Rates. As we have reported elsewhere,[18] CS_2 has rather high capability to dissolve regioregular P3BT at room temperature so as P3BT/CS_2 solutions with the concentration up to, e.g., 30 mg/mL could be prepared. The obtained solution with such a high concentration still demonstrates a lovely orange appearance, which gives strong indication that rigid P3BT molecules have been well dissolved in CS_2. It has already been suggested that the morphology of thin crystalline P3AT film deposited from its solution is strongly dependent on the corresponding solvent evaporation rate. As a general consequence, a slower solvent evaporation usually leads to higher crystallinity or/and less defects in obtained crystals.[9,11,26] Figure 1 shows morphology of the thin P3BT film as prepared from the same P3BT/CS_2 solution but with different solvent evaporation rates. The nature of fast solvent evaporation associated with the spin-coating method, together with high volatility of solvent CS_2 (having very low boil point 46 °C at 1 atm), results in very fast drying process, and thus solidification of the thin film could complete within a few seconds. Correspondingly, as shown by BF-TEM in Figure 1a, no morphological feature could be resolved from this specimen. The SAED pattern as an inset shows two discernible diffraction rings, which correspond to the reflections from crystallographic (100) and (020) planes associated with form I modification.[13,19] The rather weak reflections of (020) planes but somehow strong reflections from (100) planes hints the P3BT crystallites are mainly adopted "plane-on" orientation with their $\pi-\pi$ stacks piled up on the thin film.[2] However, short fibril (Figure 1b) dominates the main feature of the drop-cast film upon a bit increased evaporation time to ∼5 s. The corresponding SAED pattern only shows enhanced diffraction ring contributed from crystallographic (020) planes of form I.

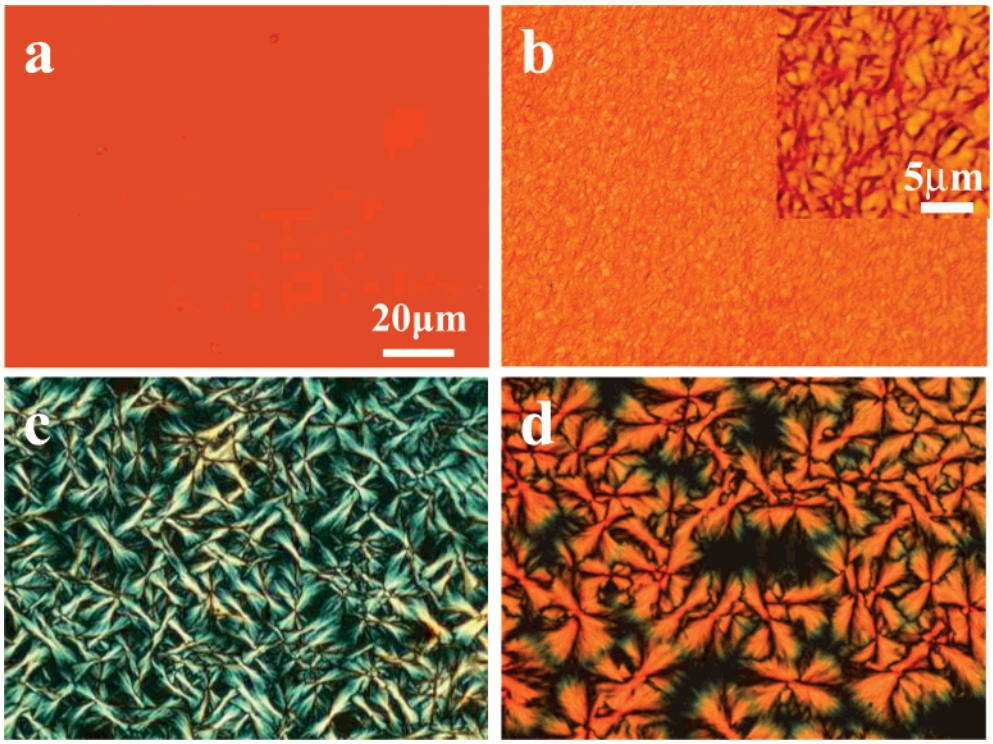

Figure 3. Optical microscopy (OM) images showing morphology of P3BT film upon CS_2 vapor treatment at different pressures for given time: (a) bright-field (BF) OM image of the pristine film spin-coated from ODCB solution; (b) BF-OM image of the film upon CS_2 vapor treatment at 0.94 for 24 h, inset is a zoom-in image showing the film is actually composed of small spherulites; (c, d), cross-polarized OM (POM) images of the film upon CS_2 vapor treatment at ∼0.96 and ∼0.98, respectively, for 12 h. All the images have the same scale bar.

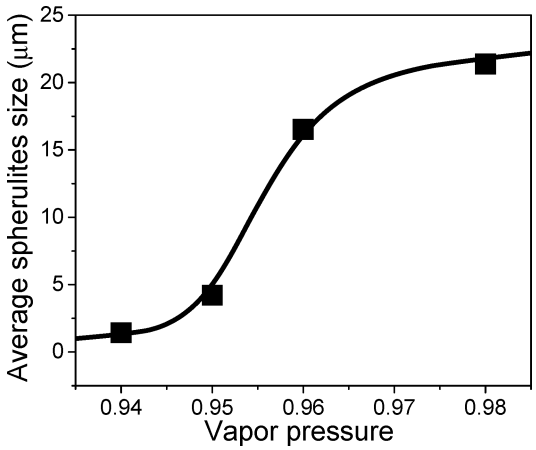

Figure 4. Dependence of average size of P3BT spherulites created in its film on the vapor pressure employed for the treatment.

The disappearance of reflections from (100) planes and significantly enhanced reflections from (020) planes imply that the P3BT crystallites in Figure 1b adopt "edge-on" orientation with their $\pi-\pi$ stacks parallel to the thin film. The different orientations of $\pi-\pi$ stacks within polythiophene crystallites with respect to the thin film have been reported on P3HT with different regioregularities or different deposition methods, where "plane-on" orientation is observed in P3HT with lower regioregularity spin-coated from chloroform.[2] However, upon further increased evaporation time and thus slower evaporation of CS_2 solvent, P3BT crystallizes into spherulites and their size is still dependent on the solvent evaporation rate (Figure 1c,d). As has already been reported by us, the lamellae of the spherulites interestingly adopt "flat-on" orientation with main P3BT backbones perpendicular to the film plane and these crystals take form II instead of I modification.[18]

As further confirmed by X-ray diffraction shown in Figure 2, the film with short solvent evaporation time (~5 s) only gives single diffraction peak at $2\theta = 6.88°$, which is corresponding to (100) reflections of form I. In contrast, for the film obtained upon a very long evaporation time of ca. 30 min, its XRD profile is mainly dominated by the diffraction peaks associated with form II P3BT crystals, accompanied by the presence of small amount of form I structure.

Upon slow solvent evaporation the concentration of polymer gradually increases until a critical supersaturation reaches, which subsequently induce nucleation of form II P3BT crystals. Similar to that of crystallization behaviors of the polymer upon cooling from the melt with different cooling rates, a relatively faster solvent evaporation rate usually generate more nuclei as a consequence of the higher supersaturation, which results in more spherulites and correspondingly smaller size. In contrast, an extremely low evaporation rate only allows generation of a few nuclei which gradually grow into very large spherulites. As the evaporation rate further increases, more nuclei are generated, which however develop into P3BT crystals with form I structure as a kinetically controlled result. This gives strong suggestion that the development of P3BT spherulite with form II modification from CS_2 solution is a thermodynamically favored process. The typical whiskerlike crystals with form I modification obtained from fast evaporation rate is however a kinetically controlled morphology. Generally, the dependence of crystalline form of obtained P3BT crystals on the solvent evaporation rate should be relevant to the thermodynamic stability of the various forms directly crystallized from this solvent. Therefore, we doubt whether the far more commonly obtained form I P3BT crystal is still the thermodynamically stable form compared with form II from solvent CS_2.

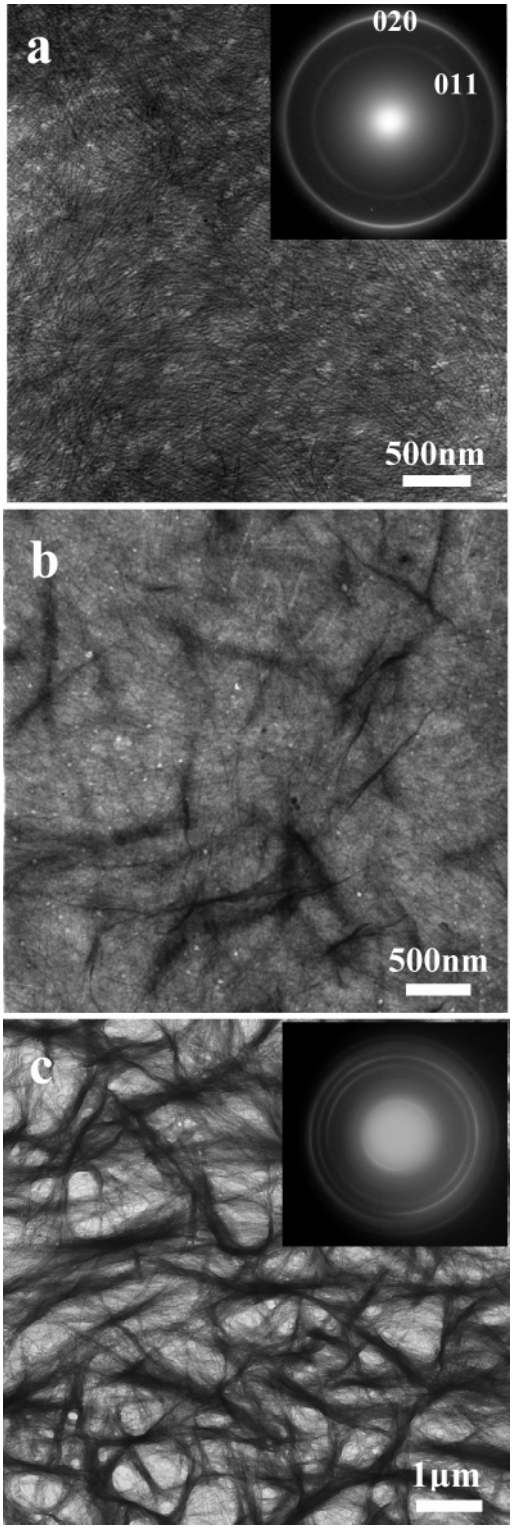

Figure 5. BF-TEM images showing gradual transition process with time of P3BT film from form I to II upon CS_2 treatment at relatively low vapor pressure $p = 0.94$: (a) pristine film spin-coated from ODCB solution; (b, c) treated for 8 and 24 h, respectively. Insets are corresponding SAED patterns.

2. Morphology and Phase Evolution of P3BT upon Controlled Solvent Vapor Treatment. As has already been pointed out in our previous publication,[18] although the different crystal forms of P3BT could be obtained through controlling the solvent evaporation rate, the large-scale homogeneity of the

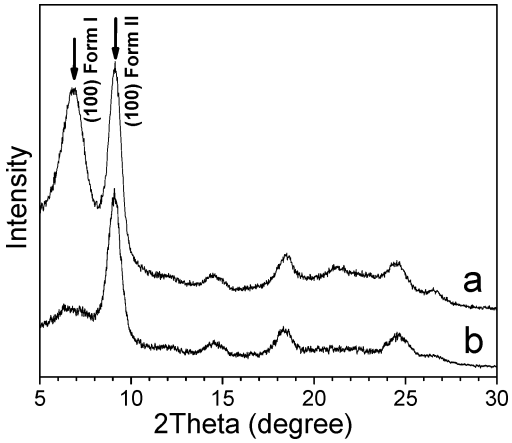

Figure 6. WAXD profile of P3BT film upon CS_2 vapor treatment at $p = 0.94$ for 24 h (a) and $p = 0.96$ for 24 h (b).

thin film cannot be ensured due to the intrinsic disadvantage of sample preparation via static casting. Therefore, it would be better to have the homogeneous thin films first prepared by spin-coating. These films are then undergone solvent vapor treatment[18,27−31] with controlled vapor pressure and treatment time (here we call it "controlled solvent vapor treatment" (C-SVT)), which entitles the samples with different morphology including crystallinity, crystallographic structure, and orientation of these crystals in the thin film. For the convenience, here we use a combination (p, t) to describe the detailed parameters used during the C-SVT process in this work, where p represents CS_2 vapor pressure and t represents the treatment time (Scheme 1).

Homogeneous thin P3BT film could be easily obtained via the spin-coating method from its *o*-dichlorobenzene (ODCB) solution, as verified by optical microscopy and TEM shown in Figure 3a and Figure 5a, respectively. These thin films are actually composed of long whiskerlike crystals[19,32,33] of P3BT with homogeneous distribution throughout the whole film. The spherulite of P3BT is subsequently achieved upon exposure to solvent CS_2 vapor. The size of these spherulites is nevertheless dependent on the solvent vapor pressures applied. As shown in Figure 3b, spherulites with rather small size around 2 μm are obtained from the film treated at (0.94, 24 h). However, these small and even immature spherulites throughout the whole film endow the thin film with integrity and homogeneity within large area. The spherulites could be increased to ca. 15 and 20 μm in higher vapor pressures, e.g., (0.96, 12 h) and (0.98, 12 h), respectively, as employed for the treatments. Figure 4 gives the plot of average diameters of P3BT spherulites obtained vs the

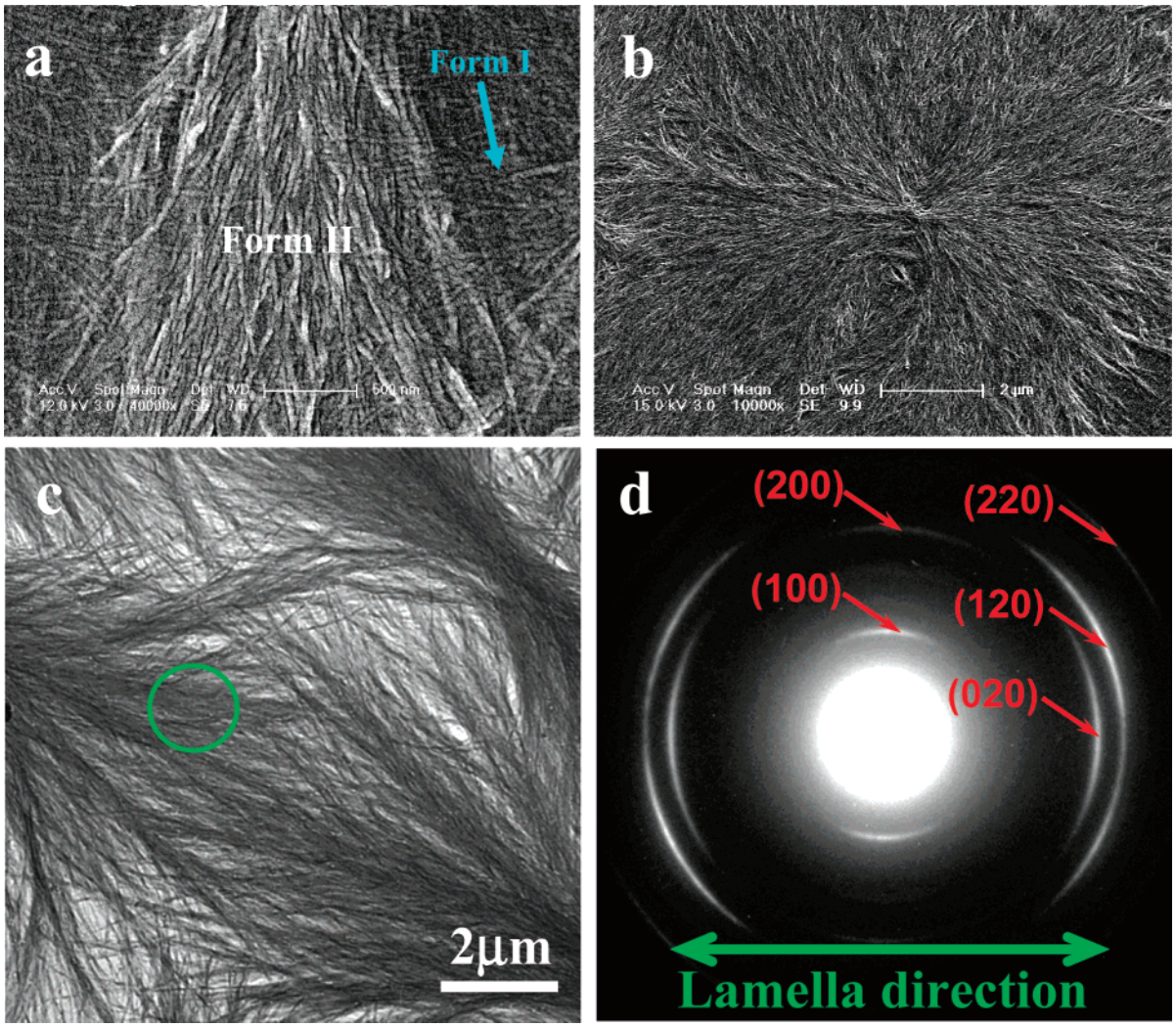

Figure 7. Scanning electron microscopy (SEM) and TEM images showing evolution process of P3BT crystals from form I to II modification upon CS_2 treatment at elevated vapor pressure $p = 0.96$. (a) SEM image demonstrating the coexistence of the two modifications in the film after a treatment of 4 h. (b) SEM image showing a complete morphology of a spherulite after 12 h treatment, which hints the transition has almost completed. (c) TEM image and corresponding SAED pattern (d) confirm the crystal structure of form II and orientation of lamellae associated with the spherulite.

vapor pressure applied during the treatment. The increased vapor pressure on the one hand enhances mobility of P3BT molecules within the film and, on the other hand, results in more solvent molecules absorbed into the film, and only those nuclei larger than critical size of form II could survive and eventually grow up into larger spherulites, as suggested by the Kelvin (or Gibbs−Thomson) equation.[34,35] Consequently, the size of achieved P3BT spherulites increases with CS_2 vapor pressure used for the treatment.

The transition mechanism from whiskerlike crystals to lamellae associated with the spherulites upon solvent vapor treatment could be interpreted in terms of crystal nucleation and growth. Microscopically, this transition is actually carried out via reorganization or recrystallization process with the presence of solvent CS_2, which should be strongly related to the different stability (solubility) of forms I and II in the solvent. Anyway, form I of P3BT crystals should be dissolved first upon exposed to the solvent vapor, followed by the formation of form II crystals. However, no phase transition could be observed at vapor pressure $p < 0.94$, which hints that P3BT crystals in form I are not dissolved by the vapor and this form is still the stable one at this vapor pressure.

To further illuminate the detailed morphology evolution process during the treatment, Figure 5 gives TEM micrographs of the thin films upon vapor exposure for different times at vapor pressure $p = 0.94$, which is the minimum pressure to induce this transition. Upon a treatment of 8 h, P3BT spherulites have nucleated as their nuclei randomly dispersed in the thin film with background of form I whiskers (Figure 5b). After a treatment of 24 h, P3BT spherulites with a size of 1−4 μm appear on the film. However, as also shown on this image, there are still certain amount of whiskerlike form I crystals staying together with these spherulites. X-ray diffraction profile (Figure 6a) confirms that both form I and II crystals are actually coexistent upon the treatment at (0.94, 24 h). By resorting to the Debye−Scherrer equation, the crystal size along given crystallographic planes could be estimated. Correspondingly, the size along crystallographic *a*-axis (or [100] direction) for both the original whiskerlike crystals in form I and new developed spherulites are determined to be 4.6 and 13.2 nm, respectively. This result again confirms that the size of form II P3BT crystals is much larger than that of form I,[18,36] as directly evidenced along the [100] direction using TEM and AFM measurements.

However, P3BT is able to nucleate and grow toward form II crystals within shorter time of 4 h at slightly elevated vapor pressure $p = 0.96$. As shown by SEM in Figure 7a, the overlapping between whiskers of form I crystals and the nucleated spherulites of form II on the thin film can be clearly observed, as indicated by the arrows inserted. As treatment time is increased to 12 h, those spherulites grow up by depleting form I whiskers surrounded and eventually no remaining whiskers can be obviously observed (Figure 7b). TEM observation on thus obtained spherulites (Figure 7c) shows their much more pronounced lamellae individually than those lamellae obtained upon a treatment at $p = 0.94$, as shown in Figure 5c. The corresponding electron diffraction pattern (Figure 7d) confirms the majority of the lamellae adopt flat-on orientation with respect to the film plane and these lamellae grow along crystallographic *b*-axis. As further proved by the X-ray diffraction profile given in Figure 6b, the P3BT film experienced a treatment at vapor pressure $p = 0.96$ for 24 h has already resulted in almost complete transition from form I to II modification.

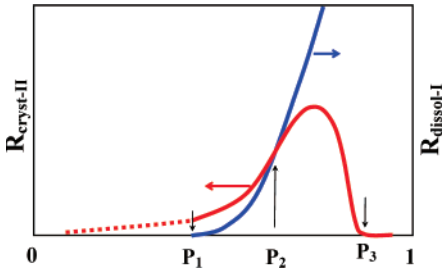

Figure 8. Schematic illustration showing the dependence of crystallization rate of form II ($R_{cryst-II}$) and dissolution rate of form I ($R_{dissol-I}$) on the vapor pressure. P_1 denotes the starting dissolution point of form I. At P_2, $R_{cryst-II} = R_{dissol-I}$; P_3 denotes the dissolution point of crystals at any forms. For P3BT treated by CS_2 vapor at room temperature, $P_1 \approx 0.94$, $P_2 \approx 0.96-0.98$, and $P_3 \approx 0.98-1.0$, as determined in this work.

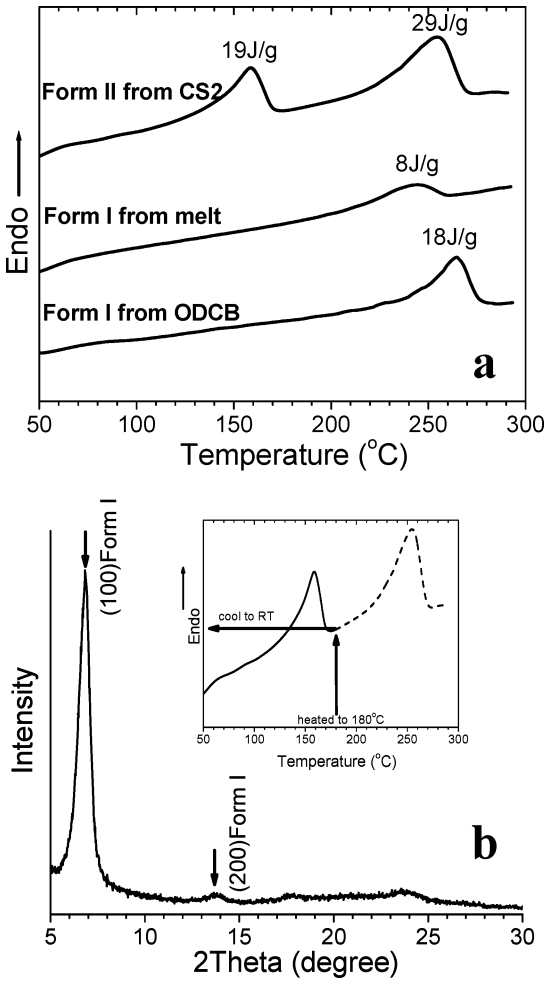

Figure 9. (a) DSC heating thermograms of P3BT crystals slowly crystallized from CS_2 solution (upper trace), a second heating trace after cooling down to room temperature from the melt (middle trace), and P3BT crystals crystallized directly from ODCB solution (lower trace). (b) XRD profile showing form I modification of P3BT crystals, which is initially prepared via slow solvent evaporation from CS_2 solution, followed by heating to 180 °C and finally cooled to room temperature. Inset shows sample preparation scheme.

Therefore, for the treatment employed vapor pressure below $p = 0.94$, almost no transition could be observed. For the treatments with vapor pressures in between $p = 0.94$ and 0.96, the transition from I to II modification does take place, which even could be a complete transition provided that long enough time is given. Nevertheless, for the treatments performed at too high vapor pressure, e.g., $p > 0.98$, any forms of P3BT crystals will be definitely dissolved by the too much solvent absorbed

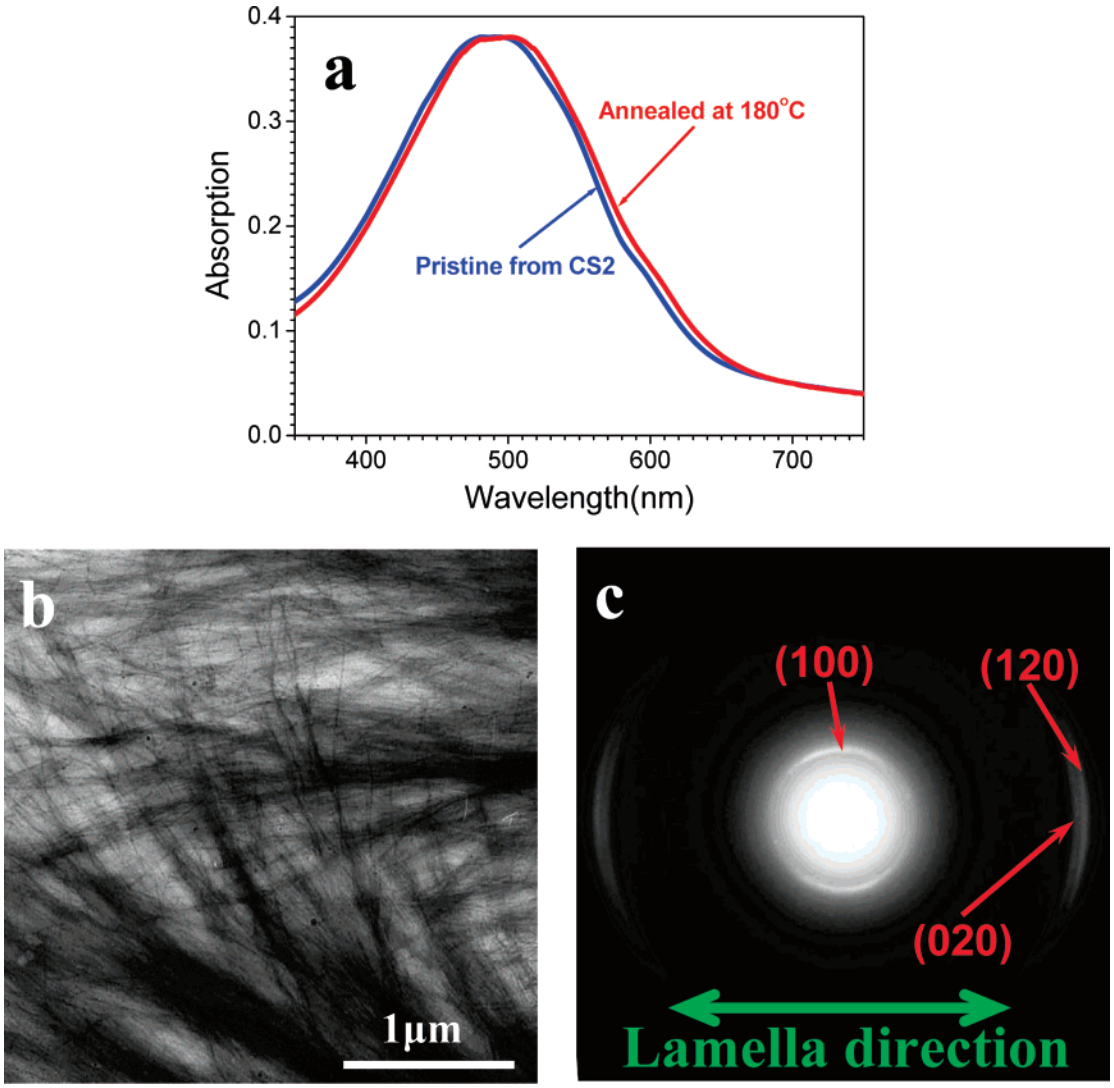

Figure 10. (a) Comparison of UV−vis absorption spectra of the same P3BT film composed of form II crystals obtained via solvent vapor treatment and of form I crystals transferred from form II upon cooling from 180 °C to room temperature. (b) Bright-field TEM image and (c) corresponding SAED pattern of form I P3BT crystals, obtained from form II upon heating. SAED pattern reveals that the P3BT lamellae adopt a flat-on orientation and $\pi-\pi$ stacking (020) (shown by arrow) is along elongated direction of the crystals.

on the samples. As a result, the homogeneity of the film will be completely destroyed resulted from the dewetting between the film and substrates as the occurrence of an instability associated with the thin liquid film, e.g., Rayleigh instability.[37−39]

To rationalize this strong dependence of the crystallographic transition on solvent vapor pressure applied, those parameters including dissolution of form I crystals and crystallization of form II crystals from the solution are introduced for consideration. It is correspondingly proposed that this transition has to be initially induced by the dissolution of form I in the solvent. As shown in Figure 8, the crystallization rate of form II ($R_{cryst-II}$) is assumed to be increased with vapor pressure at low vapor pressure. Despite of much high stability of form II crystal in CS_2 vapor, it will be eventually dissolved at extremely high vapor close to saturated pressure. Therefore, for the treatment with vapor pressure in between P_1 and P_2, form I crystals are gradually dissolved, and those dissolved part simultaneously transits to II modification. For vapor pressure higher than P_2, form I is dissolved completely within a very short time, and thus a thin liquid layer is first obtained, followed by crystallization of P3BT from the solution, and eventually form II modification is achieved. Vapor pressure point P_3 is a critical value where $R_{cryst-II} = 0$. P3BT crystals in any modifications will be dissolved with further increased vapor pressure above P_3, which is very close to the saturated vapor pressure of CS_2 at room temperature.

As a post-treatment method particularly suitable for thin film to carry out morphology optimization, both the appropriate vapor pressure and treatment time depending on the materials involved in the thin film should be deliberately chosen so as to carry out the treatment. These considerations are highly comparable to another much popular treatment method thermal annealing, where annealing temperature and time should be also predetermined according to the melting point of the materials. Similarly, one of the most important criterions to choose an appropriate vapor pressure is the stability (or solubility) of the material (or its specific phase) in the solvent. For instance, the thin regioregular poly(3-hexylthiophene) (P3HT) film starts to dissolved in CS_2 vapor at $p = 0.73$ where the film color gradually changes from dark purple to orange. This dissolution point ($p \approx 0.73$) is much lower than that of P3BT ($p > 0.98$) because of longer substituted side chain on the main polythiophene backbone, which leads P3HT more easily to be dissolved by CS_2 even in the same crystalline state.

3. Reverse Phase Transition of Form II Back to I Modification upon Heating. As a relatively thermodynamically

stable form prepared from slowly evaporated CS_2 solution or upon solvent CS_2 vapor treatment, the thermodynamic behavior of form II P3BT crystal upon heating process could reflect whether this observed behavior is only valid for the behavior from the solution by using solvent CS_2 or a general characteristics of form II in the all cases including thermodynamics in its bulk state without any solvent. As shown in Figure 9a, DSC heating curves of form II P3BT crystals as prepared from slowly evaporated CS_2 solution shows two endothermic transitions with $\Delta H = 19$ J/g and 29 J/g, respectively. XRD profile has confirmed the pristine sample is mainly composed of form II crystals. Therefore, the first endothermic peak at heating trace should be attributed to a phase transition. For the samples prepared from ODCB solution or from melt crystallization, only an endothermic peak around 250 °C which is associated with the melting temperature of P3BT crystals (form I) is observed. To further disclose this transition around 159 °C of form II, the sample was heated to 180 °C, where the transition has completed. Afterward, the sample was cooled to room temperature and investigated by XRD. As shown in Figure 9b, the sample has completely transferred back to form I modification. This experiment clearly confirmed that the transition on the heat trace is actually a solid−solid phase transition of II to I modification.[23] The fact that transition of form II to I modification at about 159 °C during heating process has forced us to draw a conclusion that the thermodynamically stable form of P3BT at room temperature is its form II modification instead of far more commonly obtained form I crystals. This fact is not only valid for the specimen prepared CS_2 solution as we have proposed,[18] but also in its bulk state without any solvent.

Although a solid−solid phase transition takes place around 159 °C and the form II P3BT crystals in the thin film sample has transfer back to form I, almost no obvious change is found in its optical absorption (to be precise, only a less than 5 nm red shift for the heated sample), as shown in Figure 10a. The TEM image (Figure 10b) and corresponding in-situ SEAD pattern (Figure 10c) show the thin film is sill composed of spherulites with rather high crystallinity, and P3BT lamellae still adopt a flat-on orientation relative to the film plane, as that of form II crystals obtained via solvent vapor treatment.

Conclusion

In summary, we have shown morphology of thin P3BT film with different crystallographic forms and solvent/thermal induced phase transition between conventional forms I and II by using, e.g., POM, TEM, SEM, DSC, and XRD. Form I modification of P3BT, which is the most frequently observed phase with typical whiskerlike morphology, is directly deposited from CS_2 solution with fast solvent evaporation. In contrast, slow solvent evaporation from CS_2 solution results in P3BT crystals in form II modification. Form I will be gradually transferred to form II upon controlled solvent vapor treatment by using CS_2. This transition is actually induced by the different stability of the two modifications in the solvent CS_2. At elevated temperature, form II crystals transfer back to form I at about 159 °C via a solid−solid phase transition. The transition behaviors of P3BT crystals upon both solvent vapor treatment and thermal heating at its bulk state reveals that form II instead of far more commonly observed form I modification is the thermodynamically stable structure for P3BT at room temperature. Although so far form II can only be obtained by using CS_2 as a solvent via slow solvent evaporation or vapor treatment, the much larger crystal size associated with this less studied crystalline structure compared with form I might significantly increase the property of this polythiophene. The solid−solid transition at elevated temperature from type II to I structure could also be employed to fabricate form I crystals eventually with high crystallinity and flat-on lamellae orientation in the thin film via constructing highly crystalline form II modification as the initial state.

Acknowledgment. This work was supported by National Natural Science Foundation of China (Grant No. 20604029). X.Y. thanks the Fund for Creative Research Groups (Grant No. 50621302) for financial support.

References and Notes

(1) Friend, R. H.; Gymer, R. W.; Holmes, A. B.; Burroughes, J. H.; Marks, R. N.; Taliani, C.; Bradley, D. D. C.; Dos, Santos, D. A.; Brédas, J. L.; Lögdlund, M.; Salaneck, W. R. *Nature (London)* **1999**, *397*, 121.
(2) Sirringhaus, H.; Brown, P. J.; Friend, R. H.; Nielsen, M. M.; Bechgaard, K.; Langeveld-Voss, B. M. W.; Spiering, A. J. H.; Janssen, R. A. J.; Meijer, E. W.; Herwig, P.; Leeuw, D. M. d. *Nature (London)* **1999**, *401*, 685.
(3) Yu, G.; Gao, J.; Hummelen, J. C.; Wudl, F.; Heeger, A. J. *Science* **1995**, *270*, 1789.
(4) Ling, M. M.; Bao, Z. *Chem. Mater.* **2004**, *16*, 4824.
(5) Coakley, K. M.; McGehee, M. D. *Chem. Mater.* **2004**, *16*, 4533.
(6) Bao, Z.; Dodabalapur, A.; Lovinger, A. J. *Appl. Phys. Lett.* **1996**, *69*, 4108.
(7) Yang, X. N.; Loos, J.; Veenstra, S. C.; Verhees, W. J. H.; Wienk, M. M.; Kroon, J. M.; Michels, M. A. J.; Janssen, R. A. J. *Nano Lett.* **2005**, *5*, 579.
(8) Huynh, W. U.; Dittmer, J. J.; Alivisatos, A. P. *Science* **2002**, *295*, 2425.
(9) Yang, H.; Shin, T. J.; Yang, L.; Cho, K.; Ryu, C. Y.; Bao, Z. *Adv. Funct. Mater.* **2005**, *15*, 671.
(10) Goffri, S.; Müller, C.; Stingelin-Stutzmann, N.; Breiby, D. W.; Radano, C. P.; Andreasen, J. W.; Thompson, R.; Janssen, R. A. J.; Nielsen, M. M.; Smith, P.; Sirringhaus, H. *Nat. Mater.* **2006**, *5*, 950.
(11) Li, G.; Shrotriya, V.; Huang, J.; Yao, Y.; Moriarty, T.; Emery, K.; Yang, Y. *Nat. Mater.* **2005**, *4*, 864.
(12) Kim, J. Y.; Lee, K.; Coates, N. E.; Moses, D.; Nguyen, T.-Q.; Dante, M.; Heeger, A. J. *Science* **2007**, *317*, 222.
(13) Chen, S. A.; Ni, J. M. *Macromolecules* **1992**, *25*, 6081.
(14) Chen, T.-A.; Wu, X.; Rieke, R. D. *J. Am. Chem. Soc.* **1995**, *117*, 233.
(15) Lu, G. H.; Tang, H. W.; Qu, Y. P.; Li, L. G.; Yang, X. N. *Macromolecules* **2007**, *40*, 6579.
(16) Pandey, S. S.; Takashima, W.; Endo, T.; Rikukawa, M.; Kaneto, K. *Synth. Met.* **2001**, *121*, 1561.
(17) Park, Y. D.; Kim, D. H.; Jang, Y.; Cho, J. H.; Hwang, M.; Lee, H. S.; Lim, J. A.; Cho, K. *Org. Electron.* **2006**, *7*, 514.
(18) Lu, G. H.; Li, L. G.; Yang, X. N. *Adv. Mater.* **2007**, *19*, 3594.
(19) Ihn, K. J.; Moulton, J.; Smith, P. *J. Polym. Sci., Part B: Polym. Phys.* **1993**, *31*, 735.
(20) Kim, D. H.; Jang, Y.; Park, Y. D.; Cho, K. *Macromolecules* **2006**, *39*, 5843.
(21) Kim, D. H.; Jang, Y.; Park, Y. D.; Cho, K. *J. Phys. Chem. B* **2006**, *110*, 15763.
(22) Zen, A.; Saphiannikova, M.; Neher, D.; Grenzer, J.; Grigorian, S.; Pietsch, U.; Asawapirom, U.; Janietz, S.; Scherf, U.; Lieberwirth, I.; Wegner, G. *Macromolecules* **2006**, *39*, 2162.
(23) Prosa, T. J.; Winokur, M. J.; McCullough, R. D. *Macromolecules* **1996**, *29*, 3654.
(24) Meille, S. V.; Romita, V.; Caronna, T.; Lovinger, A. J.; Catellani, M.; Belobrzeckaja, L. *Macromolecules* **1997**, *30*, 7898.
(25) Prosa, T. J.; Winokur, M. J.; Moulton, J.; Smith, P.; Heeger, A. J. *Macromolecules* **1992**, *25*, 4364.
(26) Ho, P. K.-H.; Chua, L.-L.; Dipankar, M.; Gao, X.; Qi, D.; Wee, A. T.-S.; Chang, J.-F.; Friend, R. H. *Adv. Mater.* **2007**, *19*, 215.
(27) Iwatsu, F.; Kobayashi, T.; Uyeda, N. *J. Phys. Chem.* **1980**, *84*, 3223.
(28) Conboy, J. C.; Olson, E. J. C.; Adams, D. M.; Kerimo, J.; Zaban, A.; Gregg, B. A.; Barbara, P. F. *J. Phys. Chem. B* **1998**, *102*, 4516.
(29) Mascaro, D. J.; Thompson, M. E.; Smith, H. I.; Bulović, V. *Org. Electron.* **2005**, *6*, 211.
(30) Gregg, B. A. *J. Phys. Chem.* **1996**, *100*, 852.
(31) Kim, S. H.; Misner, M. J.; Russell, T. P. *Adv. Mater.* **2004**, *16*, 2119.
(32) Kline, R. J.; McGehee, M. D.; Toney, M. F. *Nat. Mater.* **2006**, *5*, 222.
(33) Kline, R. J.; McGehee, M. D.; Kadnikova, E. N.; Liu, J.; Fréchet, J. M. J.; Toney, M. F. *Macromolecules* **2005**, *38*, 3312.
(34) Adamson, A. W.; Gast, A. P. *Physical Chemistry of Surfaces*, 6th ed.; Wiley-Interscience: New York, 1997.

(35) Horn, D.; Rieger, J. *Angew. Chem., Int. Ed.* **2001**, *40*, 4330.
(36) Pal, S.; Roy, S.; Nandi, A. K. *J. Phys. Chem. B* **2005**, *109*, 18332.
(37) Chandrasekhar, S. *Hydrodynamic and Hydromagnetic Stability*; Dover: New York, 1981.
(38) Quéré, D.; Meglio, J.-M. d.; Brochard-Wyart, F. *Science* **1990**, *249*, 1256.
(39) Reiter, G. *Langmuir* **1993**, *9*, 1344.

MA7026512